Hindawi
Modelling and Simulation in Engineering
Volume 2022, Article ID 2534439, 16 pages
https://doi.org/10.1155/2022/2534439

Research Article

Coupling Modeling and Adaptive Control for Piezoelectric-Actuated Positioning Stage

Liang Li, Shi-Xin Zhang, and Sheng-Jun Wen

Zhongyuan University of Technology, Zhengzhou 450007, China

Correspondence should be addressed to Sheng-Jun Wen; wsj@zut.edu.cn

Received 6 February 2022; Revised 21 July 2022; Accepted 3 August 2022; Published 2 September 2022

Academic Editor: Angelos Markopoulos

In this paper, a nonlinear coupling model with hysteresis, dynamics, and creep is proposed to describe accurately the complex characteristics of piezoelectric-actuated positioning stage, where a classic Hammerstein model in series with a fractional-order model is given. The fractional-order model is presented to express the nonlinear creep characteristics. Firstly, the Hammerstein structure model is composed of two blocks, where the former block is the classical PI model to describe the static hysteresis effects, and the latter block is the second-order discrete transfer function model to characterize the dynamic characteristics. In addition, the parameters of the coupling model are identified. Secondly, based on the built model, the inverse of fractional-order model and the inverse of PI model are implemented as the feedforward compensations, and an adaptive control is designed to adjust the tracking performance of the whole system. Finally, the effectiveness of the proposed coupling model and controllers are verified by the piezoelectric-actuated positioning experiment stage. Experimental results show that the established coupling model can accurately characterize the hysteresis, dynamics, and creep properties of the stage. Also, the results show that the tracking error is less than 0.8% at low frequency and mixed frequency.

1. Introduction

With the advancement of the era and the development of science and technology, the sub-micron-nanopositioning and control accuracy is required for modern scientific research and industrial production. The traditional actuator cannot meet the needs of precise positioning and control [1–3]. Therefore, the piezoelectric actuator has started to receive special attention and research from scholars [4–6]. It has gradually been applied in many fields that require fast response and high-precision actuate control, such as micro-positioning stage [7], fast tool servo system [8], and other high-precision fields. However, piezoceramic materials suffer from the strong hysteresis effect, lightly dynamic properties, and creep characteristics [4, 5, 9]. The above problems will seriously affect the positioning accuracy and motion accuracy of the piezoelectric-actuated positioning stage and even lead to the instability of the whole control system [7, 10, 11]. The nonlinear effect of the piezoelectric-actuated positioning stage is mainly the hysteresis, which is more than 80%.

Hysteresis is a rather complicated nonlinear process. The main phenomenon is that under the action of voltage signal, the ascending displacement curve generated by piezoelectric actuator does not coincide with the descending displacement curve, and a hysteresis loop will be formed by the existing displacement difference [12, 13]. In the current literature, the commonly used hysteresis nonlinear models are mainly divided into three categories [14]. The first category is the physical model based on physical principles, such as Jiles-Atherton (JA) model [15, 16]. The second category is the phenomenological model based on hysteresis nonlinear phenomena, for instance, Prandtl-Shlinskii (PI) model [17, 18]. The third category of model based on intelligent computing and learning mainly applies various intelligent algorithms to fit and model data, for example, SVM [19]. Since the phenomenological model does not involve the physical nature of hysteresis, that studies the relationship between input and output of hysteretic system, which widely used in the modeling of hysteresis phenomenon. Among those models, the strength of classic PI model is simple structure, few parameters, simple calculation process, and the existence of inverse models.

The creep characteristic means that when the voltage applied by the piezoelectric actuator no longer changes, the stable value of output displacement can be stable after a certain period of time. This phenomenon can be seen as a slow drift of piezoelectric-actuated positioning stage displacement after sudden changes in input voltage, which may cause positioning errors [20]. Nowadays, there are two types of mathematical modeling methods, which are commonly used to depict creep properties. One is the logarithmic model [21, 22], which belongs to the phenomenological model. The other is the finite spring-damping superposition model [23, 24]. Besides, the fractional operator is a modeling tool for a distributed parameter system with memory effect, and the creep effect of the piezoelectric-actuated positioning stage has global memory [20, 25]. However, the existing fractional-order model is complicated to obtain accurate parameters. In the literature [20], a fractional-order model is proposed by representing the PEA as resistocaptance, but only the step signal is studied. In addition, one coupled fractional-order creep and hysteresis model is established in [5]; however, only the creep effect under ultralow frequency is studied.

How to effectively suppress the inherent bad properties of piezoelectric-actuated positioning stage and achieve high-precision tracking control of it is a challenging question. In the literature [26], an inverse model open-loop control method based on scanning probe microscope was designed to suppress the hysteresis and other nonlinear characteristics of the intelligent driver. In the article [27], an adaptive neural digital dynamic surface control (DSC) scheme with the implicit inverse compensator is developed to mitigate the asymmetric hysteresis effect. In reference [9], an adaptive controller is proposed, which adopts a minimization parameterized hysteresis model to reduce the amount of computation. Literature [28] designs an adaptive predictive controller, which is based on t-S fuzzy model and has a parallel distributed form structure, and the controller parameters are adjusted online according to real-time error. It shown that the adaptive control strategy can accurately track the desired input signal, which is considered in this paper.

The main contribution of this paper is that a nonlinear mathematical model coupling with hysteresis, dynamics, and creep is proposed, which is a classic Hammerstein structure model in series with a fractional-order model. Firstly, due to the piezoelectric-actuated positioning stage is a distributed parameter system, where the creep effect exits memory effect, so the creep characteristics in this paper are described by the fractional-order operator which is suitable for the distributed system with memory properties. Secondly, the Hammerstein structural model is presented consisting of two blocks, where the static block is represented by the classic PI model, and the dynamic block is built by the second-order discrete transfer function model, which describes the hysteresis and the dynamics characteristics, respectively. Thirdly, based on the above model, the inverse compensations of the fractional-order and the PI model are obtained, and minimum variance-based adaptive control is designed to track the desired signal and reduce the error.

The remainder of this paper is organized as follows. Section 2 introduces the fractional calculus and its Grunwald-Letnikov (G-L) definition, which presents a detailed description of the coupling model in the piezoelectric-actuated positioning stage. The identification method of the coupling model parameters is given in Section 3. Section 4 designs a compound control algorithm combining feedforward and inverse compensation with adaptive control. Section 5 introduced the piezoelectric driving positioning experiment platform and verified the proposed coupling model through the experiment platform. Similarly, adaptive compound control effect is given in Section 5. Finally, Section 6 concludes this paper.

2. Piezoelectric-Actuated Positioning Stage Model

According to the literature review, the piezoelectric-actuated positioning stage has hysteresis, creep, and linear dynamics characteristics. Hysteresis exists in the total frequency domain of the positioning stage and is the main nonlinear factor. In addition to the hysteresis effect, the creep property occupies a secondary position in the low-frequency domain. In the high-frequency region, the dynamic strength is higher than creep. However, to describe the properties of piezoelectric-actuated positioning stage more accurately, the influence of dynamics cannot be ignored in low-frequency domain, and creep effect should not be neglected in high-frequency region. In this paper, a coupling nonlinear model of a piezoelectric-actuated positioning stage is proposed, which is based on the classic Hammerstein structure model in series with a fractional operator model. The Hammerstein structure model is composed of two blocks, where the former block is the classical PI model to describe the static hysteresis effects, and the latter block is a second-order discrete transfer function model to characterize the dynamic characteristics. The basic structure is shown in Figure 1.

2.1. PI Model. In this paper, the classical PI model of discrete-time is adopted. The classical PI model is a phenomenological model based on operators, which is formed by the linear superposition of finite weighted play operators or stop operators, in which the play operators have the properties of continuity, rate independence, and symmetry. In addition, the output of the play operator not only depends on the threshold and the corresponding weight but also has a relationship with its historical value.

According to the definition in [29], suppose that $C_m[0, t_E]$ is a space of piecewise monotonic continuous functions on the time interval $[0, t_E]$ for an arbitrary piece-wise monotone function $v(t) \in C_m[0, t_E]$. The time domain is divided into N subintervals, $0 = t_0 < t_1 < \cdots < t_i < \cdots < t_N = t_E$, and the function $v(t)$ is monotonically continuous on each

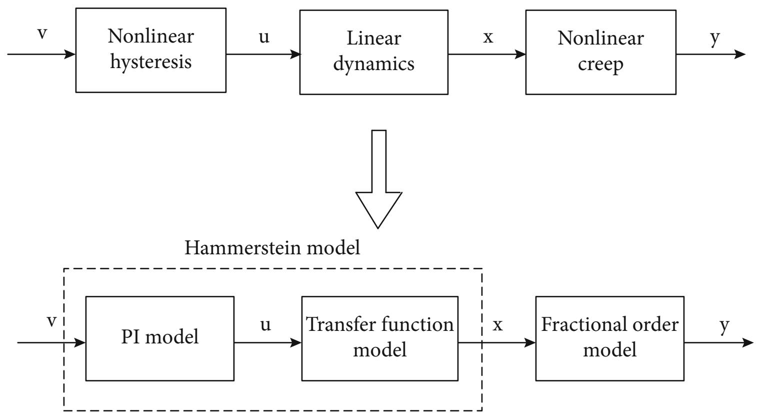

Figure 1: The proposed coupling structure model.

subinterval $[t_i, t_{i+1}]$. For the linear play operator F_r of threshold $r \geq 0$, it can be defined as

$$u(0) = F_r[v](0) = f_r(v(0), u_0), \tag{1}$$

$$u(t) = F_r[v](t) = f_r(v(t), u(t_i)), \tag{2}$$

for $t_i < t < t_{i+1}$, $0 \leq i < N$, with

$$f_r(v, u) = \max\,(v - r, \min\,(v + r, u)), \tag{3}$$

where $u(t)$ is the output of the operator. The hysteresis loop of the play operator is shown in Figure 2, which is a symmetric parallelogram shape.

The PI model of discrete time is defined by

$$P[v](t) = w_{P_0} v(t) + \sum_{j=1}^{m} w_{p_j} F_{r_j}[v](t), \tag{4}$$

for $t \in [0, t_E]$, $j = 1, 2, \cdots, m$, where m represents the number of the play operators, w_{p_j} is the weight of the play operator that is generally calculated from the experimental data and satisfies $w_{p_j} > 0$, w_{P_0} is a positive constant, and r_j is the threshold of the play operator.

In general, the selection principle of threshold r_j is to select at equal intervals, which is expressed as

$$r_j = \frac{j-1}{m} \max |v(k)|. \tag{5}$$

It should be noted that the accuracy of the PI model had much relatedness among the number of operators, which will be improved with the increase in the number of operators. However, the computation complexity increases with the number of operators, and the computation time will also increase significantly, causing severe problems in real-time applications. Therefore, it is very important to select the appropriate number of operators, and that should be a compromise e between the accuracy of the PI model and the speed of operation. After several tests, the number of operators selected in this paper is $m = 9$.

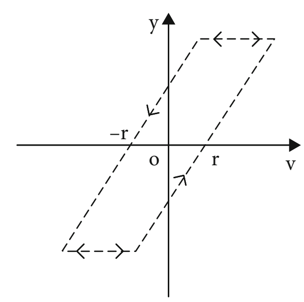

Figure 2: Play operator.

2.2. Transfer Function Model. In this section, the dynamics of the piezoelectric-actuated positioning stage will be derived. The piezoelectric-actuated positioning stage is mainly composed of a piezoelectric actuator, a flexible hinge, and a base, among which the piezoelectric actuator is the main driving element. Due to the special material properties of the piezoelectric-actuated positioning stage, its linear dynamic can be equivalent to the classical mass-spring-damping mechanism system. Under the action of the input voltage signal, the piezoelectric actuator can be regarded as a force generator that generates force, and the mechanical movement is performed through the linkage of the flexible hinge. At this time, a smaller displacement will be output by the positioning stage. Thus, the linear dynamic of the piezoelectric-actuated positioning stage can be expressed as [29]

$$M\ddot{x}(t) + B_1\dot{x}(t) + B_2x(t) = F(t), \tag{6}$$

where $x(t)$ is the output displacement of the positioning stage, $F(t)$ is the force generated by the piezoelectric actuator, M is the equivalent mass of the positioning stage, B_1 is the equivalent viscous friction coefficient of the positioning stage, and B_2 is the equivalent stiffness coefficient of the piezoelectric positioning stage.

In general, in the process of experiment and simulation, the discrete expression of linear system is usually used:

$$A\left(z^{-1}\right)x(k) = B\left(z^{-1}\right)u(k) + \varepsilon(k), \tag{7}$$

where $\varepsilon(k)$ is the error and $u(k)$ is the output of the PI model and satisfies $u(k) = F(k)$.

$$A\left(z^{-1}\right) = 1 + a_1 z^{-1} + a_2 z^{-2}, \tag{8}$$

$$B\left(z^{-1}\right) = b_1 + b_2 z^{-1}, \tag{9}$$

where z^{-1} is the unit delay shift operator, $A(z^{-1})$ and $B(z^{-1})$ are polynomials, and a_i and b_i are the coefficients of the polynomial $A(z^{-1})$ and $B(z^{-1})$, $i = 1, 2$.

The discrete transfer function is given by

$$G\left(z^{-1}\right) = \frac{B\left(z^{-1}\right)}{A\left(z^{-1}\right)}. \tag{10}$$

In this paper, let $v(k)$ was exploited as the input voltage of the positioning stage, $F(k)$ is the force generated by the piezoelectric actuator, and $P[v](k)$ is the output of the hysteresis that was given in the previous section. Then, express the relation between $F(k)$ and $P[v](k)$ as

$$F(k) = P[v](k). \tag{11}$$

2.3. Fractional-Order Model. In this section, fractional calculus is briefly introduced firstly. Fractional calculus is the generalization of basic calculus operators from integer-order to noninteger-order, and its operator ${}_{t_0}D_t^{\alpha}$ is basically defined as [30]

$${}_{t_0}D_t^{\alpha} = \begin{cases} d^{\alpha}/dt^{\alpha} & \text{Re}\ (\alpha) > 0, \\ 1 & \text{Re}\ (\alpha) = 0, \\ \int_{t_0}^{t} (d\tau)^{-\alpha} & \text{Re}\ (\alpha) < 0, \end{cases} \tag{12}$$

where t_0 is the lower limit of calculus, t is the upper limit of calculus, α is the order of calculus, which can be a complex number, and Re (α) is the real part of the order α.

In the existing literature, there are two definitions of fractional calculus that are cited most frequently, namely, Grunwald-Letnikov (G-L) definition and Riemann-Liouville (R-L) definition, respectively, wherein, the G-L definition [20, 25] of α the fractional derivative of $f(t)$ is

$$\begin{aligned} {}_{t_0}D_t^{\alpha} f(t) &= \lim_{h \longrightarrow 0} h^{-\alpha} \sum_{j=0}^{[(t-t_0)/h]} (-1)^j \binom{\alpha}{j} f(t - jh) \\ &\approx \lim_{h \longrightarrow 0} h^{-\alpha} \sum_{j=0}^{[(t-t_0)/h]} w_j^{(\alpha)} f(t - jh), \end{aligned} \tag{13}$$

where $[(t - t_0)/h]$ is the integer part and

$$w_0^{(\alpha)} = 1, w_j^{(\alpha)} = \left(1 - \frac{\alpha + 1}{j}\right) w_{j-1}^{(\alpha)}, \quad j = 1, 2, \cdots. \tag{14}$$

The Laplace transform of α fractional derivative [30] is given by

$$\mathscr{L}\left[f^{(\alpha)}(t)\right] = s^{\alpha} F(s), \tag{15}$$

for $f(t) = 0, \forall t < 0$.

The term creeps originated from the study of mechanical materials. The creep of the piezoelectric material refers to the rearrangement of its crystal grains after a period of time when the input voltage is applied, and the displacement during this period time is called creep. Besides, creep has memory properties, which is a recovery phenomenon of piezoelectric actuators in the absence of an external input return signal. It has a slow output process and can be regarded as a nonlinear process with gain uncertainty and dependent on the input voltage. The fractional-order is just the tool to describe the phenomenon with memory effect and system with distributed parameters [20, 25].

Based on the foregoing facts, the creep in this paper is described as follows:

$$y_c(t) = k_c * {}_{t_0}D_t^{\alpha} x(t), -1 \leq \alpha \leq 1, \tag{16}$$

where $y_c(t)$ is the output of the creep, $x(t)$ is the output of the Hammerstein model, and the input of the creep, k_c is the gain of the fractional-order model. When $-1 \leq \alpha < 0$ the fractional operator presents integral characteristics and $0 < \alpha \leq 1$, the derivative characteristics of fractional operator is presented.

The fractional-order model is the last part of the entire system. The output $x(k)$ of the Hammerstein model can be used as the input of the fractional-order model, and the actual output displacement $y(k)$ of the positioning stage is collected. The above data is used to identify this model. In order to facilitate computer programming and industrial practice, formula (16) is discretized as

$$y_c(k) = k_c * h^{-\alpha} \sum_{j=0}^{k} w_{c_j}^{(\alpha)} x(k - j). \tag{17}$$

3. Parameter Identification

In this section, the parameters of the proposed model are identified. According to the characteristics of the model, a stepwise identification method is adopted. There are three steps. Firstly, under the conditions of low frequency, to identify the PI model, parameters employed the collected actual input voltage and output displacement; secondly, to further identify the coefficients of the second-order transfer function used the obtained PI model in the case of mixed frequencies; finally, to process the output of the obtained Hammerstein model as the input of the fractional-order model and identify the parameters of the fractional-order model.

3.1. Parameter Identification of the PI Model. According to the previous methods, when the input voltage frequency is low (less than or equal to 10 Hz), the hysteresis loop is almost unchanged of piezoelectric-actuated positioning stage, which can be approximated as having static characteristics. The sinusoidal input signal $v(t) = 10 \sin(2\pi f t) + 10$ of the positioning stage is given, and where the frequency f is 1 Hz, the output displacement $y(t)$ of the positioning stage is measured. The experimental data to identify the PI model is constituted.

For the above model (4), its discrete form is expressed as follows:

$$P[v](k) = w_{P_0} v(k) + \sum_{j=1}^{m} w_{p_j} F_{r_j}[v](k), \tag{18}$$

where $F_{r_j}[v](k)$ is the output of the play operator of the PI model and w_{p_j} is the weight corresponding to the play operator and is also the parameter to be identified.

Define $y(k)$ as the displacement output measured by the experimental positioning stage, and the error value between $y(k)$ the established PI model and the positioning stage measured

$$e_P(k) = y(k) - P(k), \tag{19}$$

where $e_P(k)$ is the error between the actual collected displacement output and the PI model output and $P(k)$ is the output of the PI model.

Based on the previous discussion, using the sum of squares of the error as the criterion function required for identification, the minimum error criterion function is defined as

$$J_{P\,\min} = \mathbf{e}_P{}^T \mathbf{e}_P. \tag{20}$$

For the purpose of identifying the parameters of the PI model, the nonlinear least square method is adopted, and the number of play operators in this paper is $m = 9$. The identification result is $w_{P_0} = 0.3344$, $w_{P_1} = 0.0714$, $w_{P_2} = 0.0322$, and $w_{P_3} = 0.0072$, and the rest of the operators have extremely small values, so they are all set to 0 here.

3.2. Parameter Identification of the Transfer Function Model. For the parameter identification of the transfer function model, the mixed frequency signals $v(t) = 6\sum_{i=1}^{3} \sin(2\pi f_i t) + 18$ is used to characterize the dynamic characteristics of the stage in a wide frequency range, and $f_1 = 5$Hz, $f_2 = 40$Hz, $f_3 = 80$Hz. The new experimental data are constituted as follows. Firstly, the control input signal is given to the piezoelectric stage, and the output $P[v](k)$ of the PI model is collected as input $u(k)$ to the transfer function model. Then, the actual output displacement $y(k)$ of the positioning stage is collected as the output of the transfer function model. The system identification toolbox of the matlab software is used to identify the parameters of the second-order transfer function in this paper. The discrete form of the second-order transfer function model of the positioning stage can be obtained as

$$G(z) = \frac{0.5954z - 0.5907}{z^2 - 1.3767z + 0.3816}. \tag{21}$$

3.3. Parameter Identification of the Fractional-Order Model. With the identified Hammerstein structure model, it is ready to identify the parameters of the fractional creep model. Like the parameter identification process of the PI model, the parameters of the fractional-order model are also identified by the nonlinear least square method.

Define $e_c(k)$ as the error between the actual output displacement of the positioning stage is collected and the output of identified Hammerstein structure model.

$$e_c(k) = y(k) - y_c(k). \tag{22}$$

The minimum error criterion function is defined as

$$J_{c\,\min} = \mathbf{e}_c^T \mathbf{e}_c. \tag{23}$$

To better characterize the creep properties of the positioning stage, the fractional parameters of each frequency and the parameters of the mixed frequency are identified in this paper, respectively. The results are shown in Table 1.

4. Adaptive Compound Control

In this paper, the inverse of PI model and the inverse of fractional-order model are connected in series to eliminate the hysteresis and creep characteristics of the system. On this basis, combined with the adaptive control based on minimum variance, the system performance is adjusted so that it can track the expected input.

4.1. Inverse Compensation Control. As a phenomenological operator model that can describe the nonlinear characteristics of hysteresis, the biggest advantage of classical PI model compared with other hysteresis models is that the classical PI model has the characteristics of analytical inverse, which is beneficial to the design of controller. The inverse obtained according to the classical PI model is still the structural form of PI model, and its parameters can be obtained by numerical calculation through the parameters of PI model.

The inverse of PI model is still the combination and superposition of a limited number of the hysteresis operators and corresponding weight coefficients. According to the formula of the PI model in the previous text, the expression of the inverse of PI model is as follows

$$P^{-1}[y](k) = w_P'^{\,T} * P_{r_P'}[v](k), \tag{24}$$

where $P_{r_h'}[v](k)$ is the hysteresis operator of the inverse of PI model, $w_P'^{\,T}$ is the weight coefficient of the hysteresis operator of the inverse of PI model, and r_P' is the threshold of the hysteresis operator of the inverse of PI model.

Table 1: Parameter identification result of fractional-order model.

Frequency (f/Hz)	Gain (k_c)	Order (α)
1	1.0463	0.0002
10	1.0497	-0.0085
20	1.0386	-0.0077
50	1.0481	-0.0098
100	1.0327	-0.0059
5/40/80	1.0172	-0.0023

The threshold selection principle of the inverse of PI model is as follows:

$$r'_{Pi} = \sum_{j=0}^{i} w_{Pj}\left(r_{Pi} - r_{Pj}\right), \quad i = 0, 1, \cdots, n, \tag{25}$$

where w_P is the weight coefficient of PI model, r_P is the threshold of PI model, and n is the number of hysteresis operators.

The weight coefficient of the inverse of PI model can be calculated by the following formula:

$$w'_{P0} = \frac{1}{w_{P0}}, \tag{26}$$

$$w'_{Pi} = \frac{w_{Pi}}{\left(w_{P0} + \sum_{j=1}^{i} w_{Pj}\right)\left(w_{P0} + \sum_{j=1}^{i-1} w_{Pj}\right)}, \tag{27}$$

where w'_{P0} and w_{P0} represent the initial weight coefficients of the inverse of PI model and PI model, respectively.

Then, the initial value of the inverse of PI model can be expressed as

$$y'_{0i} = \sum_{j=1}^{i} w_j y_{0i} + \sum_{j=1+1}^{n} w_j y_{0j}. \tag{28}$$

Similarly, according to the fractional-order model in the previous article, the formula of the inverse of the fractional-order model can be obtained as follows:

$$y_c^{-1}(t) = \frac{1}{k_c} * {}_{t_0}D_t^{-\alpha} x(t), \quad -1 \le \alpha \le 1. \tag{29}$$

4.2. Adaptive Control. Let the mathematical model of the controlled object be expressed as

$$A\left(z^{-1}\right)y(k) = z^{-d} B\left(z^{-1}\right) * c \sum_{j=0}^{k} w_{cj}^{(\alpha)} z^{-j} P[v](k), \tag{30}$$

$$c = k_c * h^{-\alpha}, \tag{31}$$

where $P[v](k)$ is the output of the PI model. $A(z^{-1}) = 1 + a_1 z^{-1} + a_2 z^{-2} + \cdots + a_{n_a} z^{-n_a}$; $B(z^{-1}) = b_1 + b_2 z^{-1} + b_3 z^{-2} + \cdots + b_{n_b} z^{-n_b+1}$. $d \ge 1$ as the pure time delay; in this case, $d = 2$.

Figure 3: Piezoelectric-actuated positioning stage.

$y(k)$ is the actual system output, and $v(k)$ is the system control input.

Then, the optimal predicted output at $(k + d)$ based on the input and output data at time k and previous time is expressed as

$$y(k+d) = \frac{G\left(z^{-1}\right)}{C\left(z^{-1}\right)} y(k) + \frac{F\left(z^{-1}\right)B\left(z^{-1}\right)}{C\left(z^{-1}\right)} * c \sum_{j=0}^{k} w_{cj}^{(\alpha)} z^{-j} P[v](k), \tag{32}$$

where $C(z^{-1}) = A(z^{-1})E(z^{-1}) + z^{-d}G(z^{-1})$, $F(z^{-1}) = B(z^{-1})E(z^{-1})$, $E(z^{-1}) = 1 + e_1 z^{-1} + e_2 z^{-2} + \cdots + e_{n_e} z^{-n_e}$, $G(z^{-1}) = g_1 z^{-1} + g_2 z^{-2} + \cdots + g_{n_g} z^{-n_g}$, $F(z^{-1}) = f_1 z^{-1} + f_2 z^{-2} + \cdots + f_{n_f} z^{-n_f}$. $n_e = d - 1$, $n_g = n_a - 1$, and $n_f = n_b + d - 1$.

In this case, select the performance indicator function as

$$J = E\left\{\left[y(k) - y_d(k)\right]^2\right\}, \tag{33}$$

where $y_d(k)$ is the expected input signal.

In combination with formulas (30), (31), and (33), the minimum variance control is

$$\tilde{v}(k) = \sum_{i=0}^{m} w'^{T}_{P} \left[\sum_{j=0}^{k} w_{cj}^{(-\alpha)} \frac{1}{c} \frac{C\left(z^{-1}\right)y_d(k) - G\left(z^{-1}\right)y(k)}{F\left(z^{-1}\right)B\left(z^{-1}\right)}\right]. \tag{34}$$

As can be seen from the above equation, the characteristic equation of the system is

$$cF\left(z^{-1}\right)B\left(z^{-1}\right) = 0. \tag{35}$$

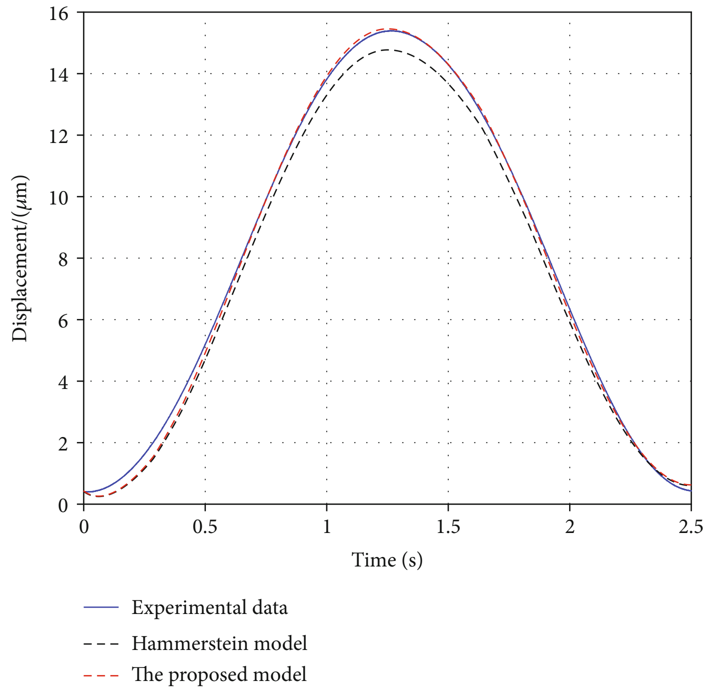

(a) $f = 1\,\text{Hz}$

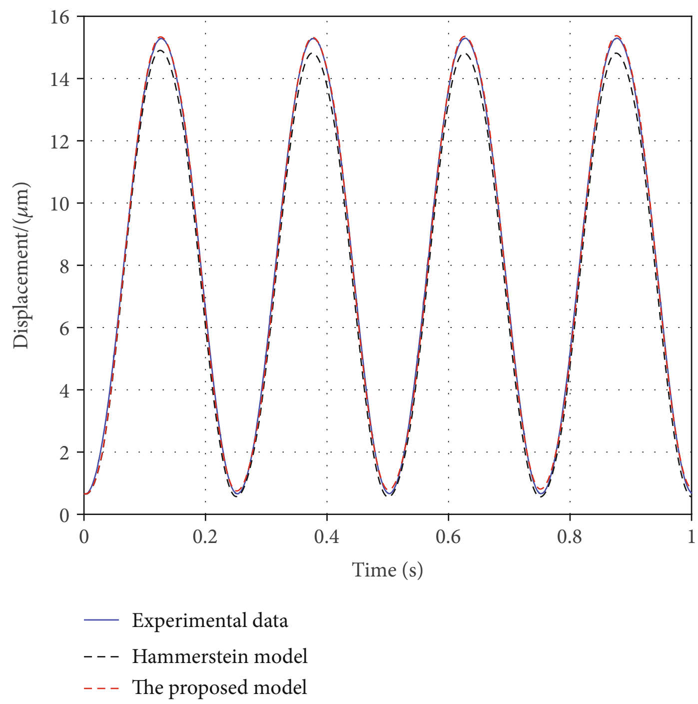

(b) $f = 10\,\text{Hz}$

Figure 4: Continued.

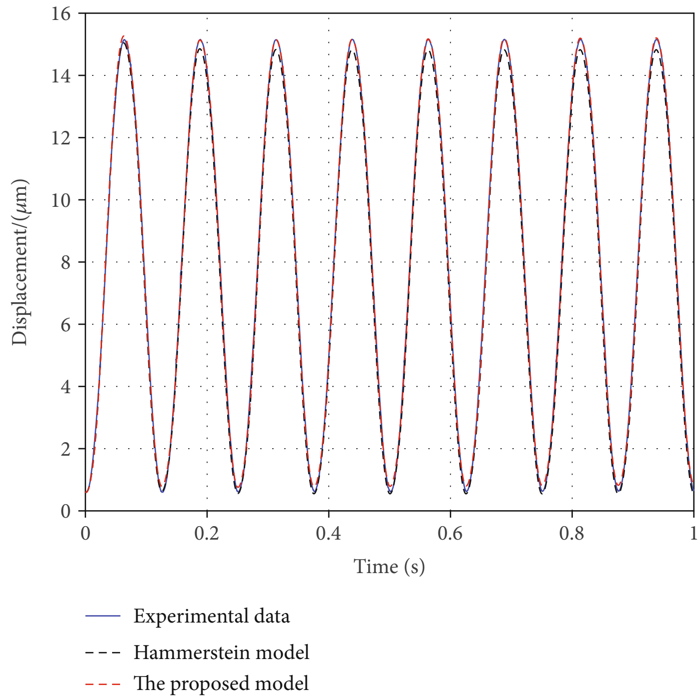

(c) $f = 20$ Hz

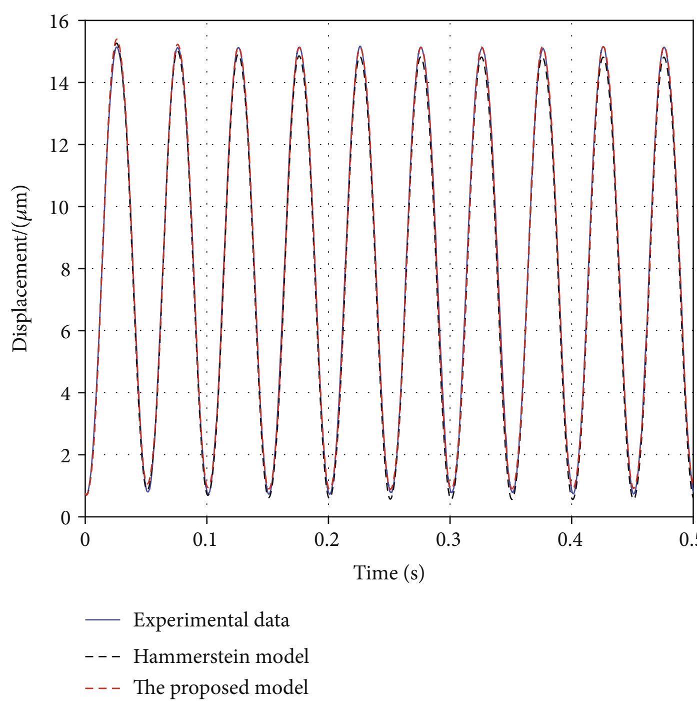

(d) $f = 50$ Hz

Figure 4: Continued.

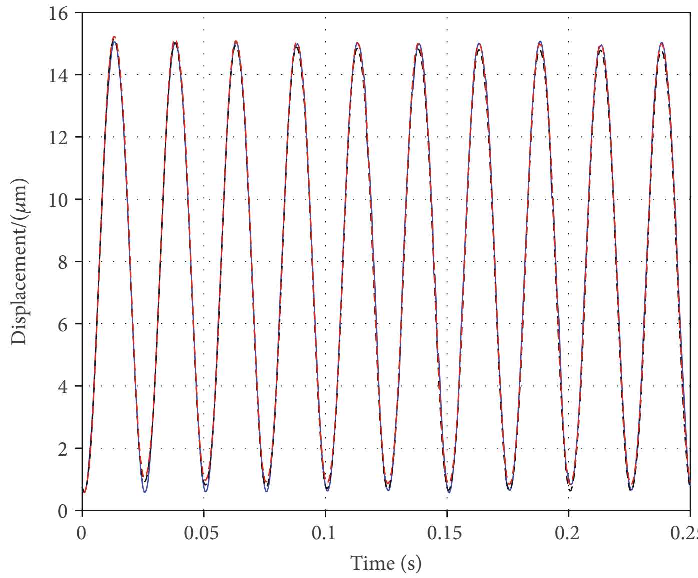

(e) $f = 100$ Hz

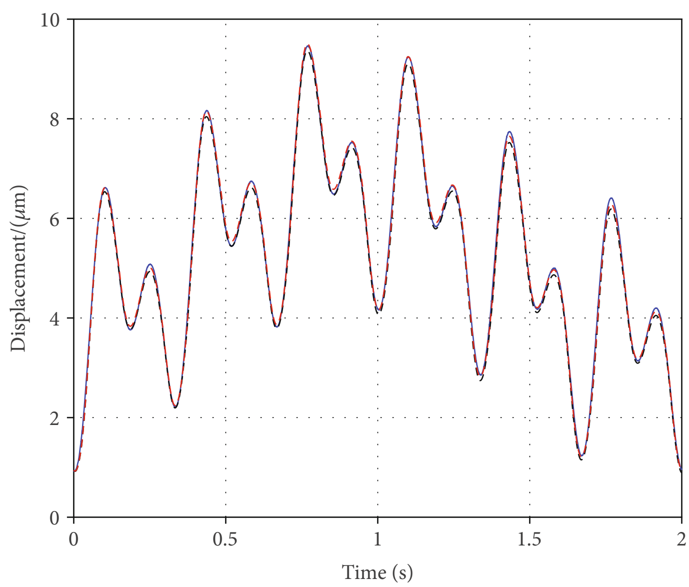

(f) $f = 5$-40-80 Hz

Figure 4: Displacement output comparison of Hammerstein model and the proposed model.

According to the characteristic equation, where c is a normal number, which does not affect the characteristics of the characteristic roots, the characteristic stability of the system is mainly determined by formula $B(z^{-1})$, and $B(z^{-1})$ is the inherent polynomial of the discrete second-order transfer function of the whole system. According to the above, it can be seen that the solutions of its equations are all in the left half-axis plane and are stable polynomials. Therefore, it can be known that the whole system is stable.

5. Simulation and Experimental Verification

5.1. Experimental Setup. In this paper, the structure of the piezoelectric-actuated positioning stage is shown in

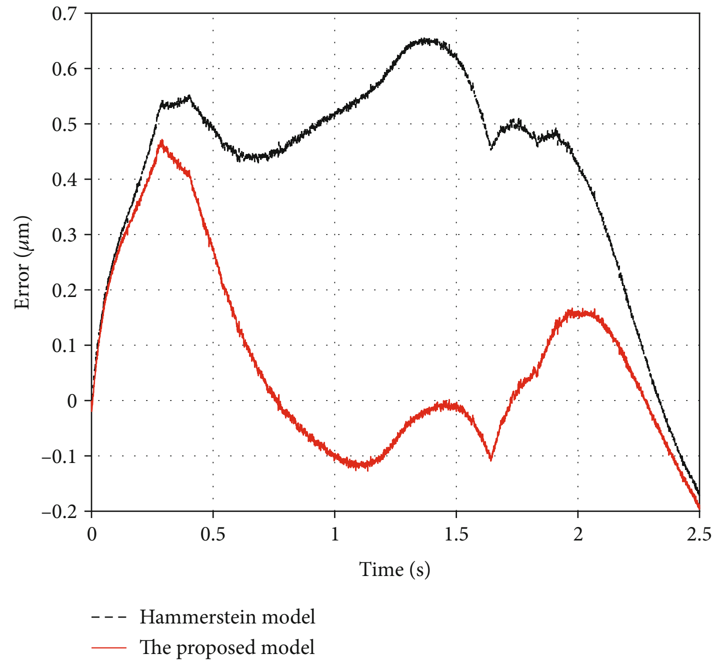

(a) $f = 1\,\mathrm{Hz}$

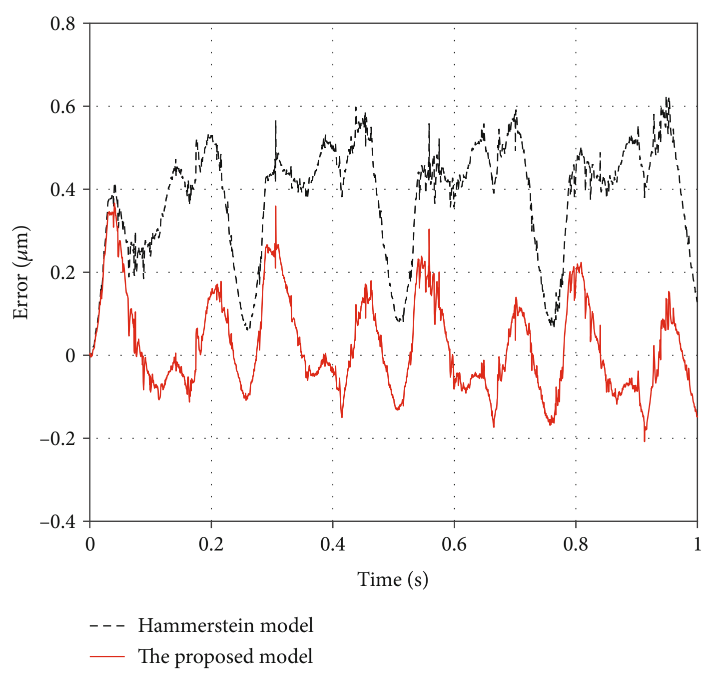

(b) $f = 10\,\mathrm{Hz}$

Figure 5: Continued.

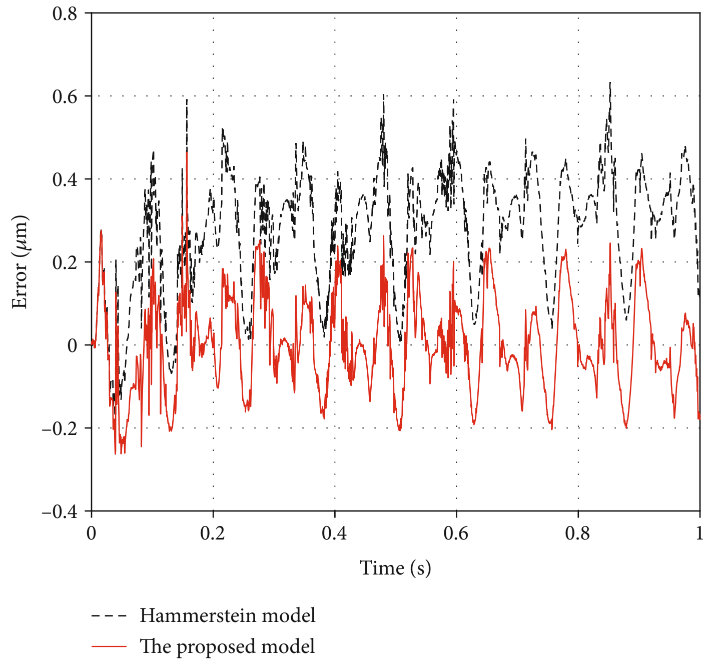

(c) $f = 20\,\mathrm{Hz}$

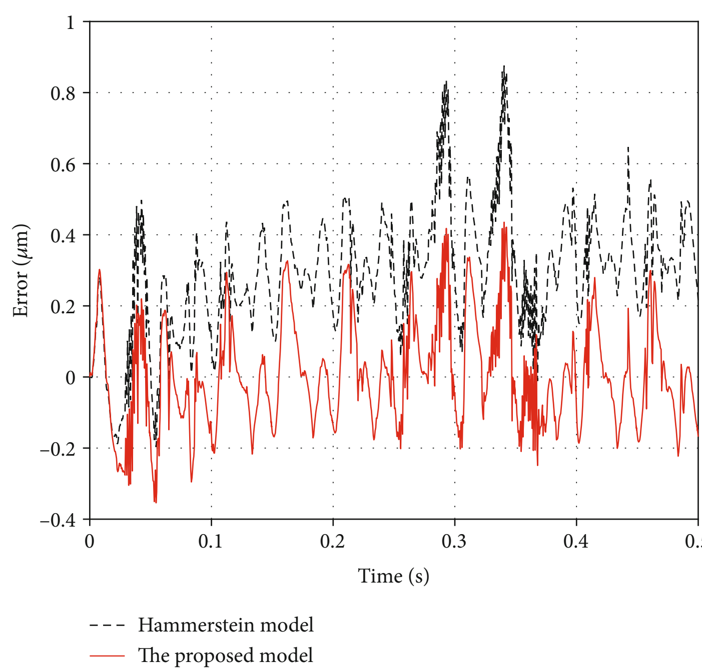

(d) $f = 50\,\mathrm{Hz}$

Figure 5: Continued.

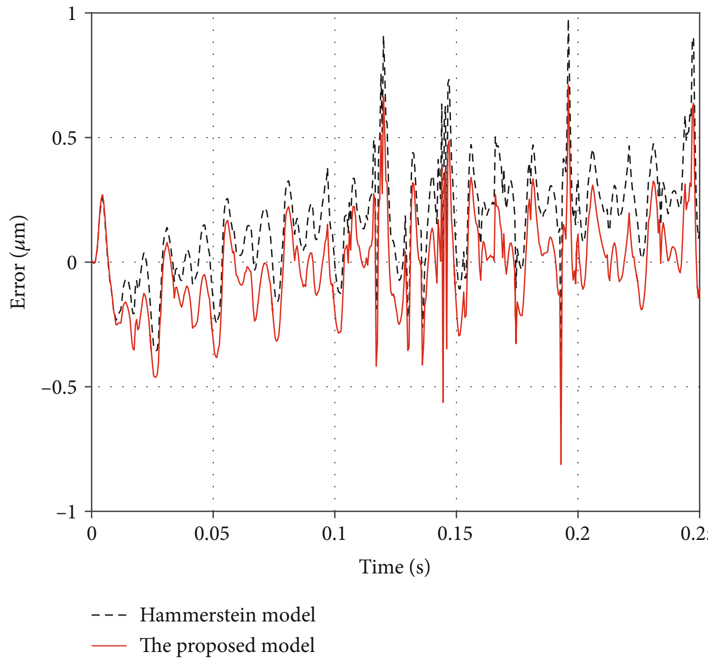

(e) $f = 100$ Hz

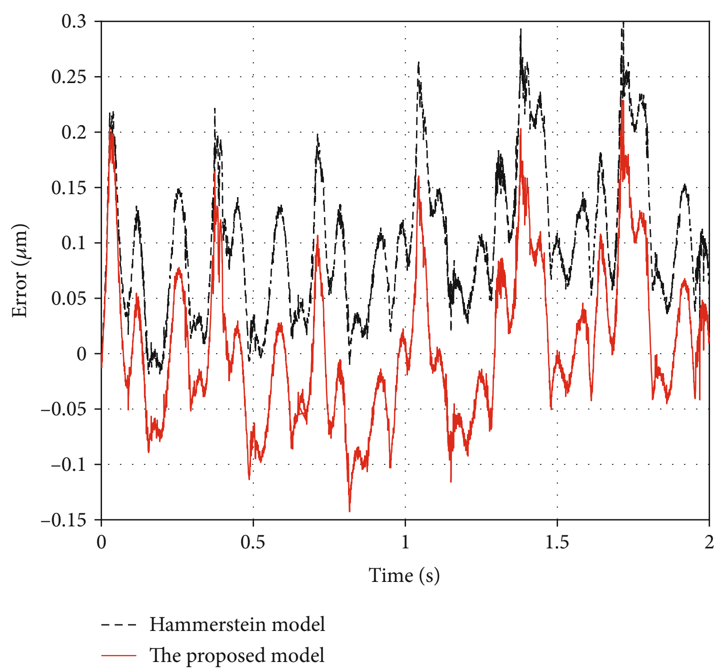

(f) $f =$ 5-40-80 Hz

Figure 5: Error analysis of Hammerstein model and the proposed model.

Figure 3. The main parts of the entire experimental system are the following. (a) Experimental piezoelectric stage PS1H80-030U, (b) piezo driver PH301, (c) signal generator SAB101, and (d) display and interface panel and experimental computer as a controller. The piezoelectric-actuated positioning stage includes a mobile stage, a piezoelectric actuator, and a displacement sensor. The resolution of the displacement sensor is 2 nm, and the maximum displacement distance of the mobile stage is 30 μm. The working process of the entire experimental system is as follows. The signal generator inputs a voltage signal of 0-10 V; after the power amplifier, the input voltage range becomes a voltage signal of 0-150 V and a bandwidth of 6 kHz, which is input to the piezoelectric driver through the display and interface panel as the driving voltage of the positioning stage, the output displacement of the positioning stage is measured by the displacement sensor, and the output displacement range is 0-100 μm after being amplified by the flexible hinge. The

signal is collected and saved by the experimental computer as the controller during the whole process. In this paper, the sampling time of the controller is 0.5 ms.

5.2. Validation and Analysis of Proposed Coupling Model. In this section, the root-mean-square error e_{rms} and the relative error e_r is employed as indicators to verify the accuracy of the model in this paper. In the following, the root-mean-square error e_{rms} and the relative error e_r are defined as

$$e_{rms} = \sqrt{\sum_{k=1}^{L} \frac{(y(k) - y_m(k))^2}{L}}, \tag{36}$$

$$e_r = \sqrt{\frac{\sum_{k=1}^{L} (y(k) - y_m(k))^2}{\sum_{k=1}^{L} (y(k))^2}}, \tag{37}$$

where L is the number of collected data, $y(k)$ is the collected displacement output of the piezoelectric-actuated positioning stage, and $y_m(k)$ is the predicted output of the proposed coupling model.

To verify the effectiveness of the proposed coupling model, experiments with a set of periodic sinusoidal voltage signals $v(t) = 10 \sin(2\pi f t) + 10$ are conducted, and the frequencies are 1 Hz, 10 Hz, 20 Hz, 50 Hz, and 100 Hz. Besides, the mixed frequency input voltage signal $v(t) = 6\sum_{i=1}^{3} \sin(2\pi f_i t) + 18$ with different frequencies $f_1 = 5\text{Hz}$, $f_2 = 40\text{Hz}$, and $f_3 = 80\text{Hz}$ also is used to excite the piezoelectric-actuated positioning stage. In this paper, the input-output characteristics of the experimental positioning stage are experimentally studied through the above two sets of input data, and the analysis conclusions will be given below.

It is well known that the positioning stage has different properties in different frequency ranges, among which the hysteresis effect always exists and is the main behavior characteristic. Besides, in the low-frequency (less than or equal to 10 Hz) range, the creep characteristics are strong, while the dynamics are weak. On the contrary, in the high-frequency (above 50 Hz) range, the dynamics are stronger than the creep properties. In the midfrequency (below 50 Hz and greater than 10 Hz) segment, the two strengths are almost the same. Nevertheless, dynamics cannot be neglected in the low-frequency range, and creep behavior cannot be ignored in the high-frequency range. Based on this fact, in order to show the effect of the coupling model more clearly, the following analysis and discussion are carried out. Figure 4 shows the experimental data of the piezoelectric-actuated positioning stage under different frequency input voltage signals and for comparison with the predicted output data of the proposed coupling model and the Hammerstein model. Figure 5 shows the fitting error of the proposed model and the Hammerstein model. It can be seen that in the low-frequency band, the creep phenomenon presented is obviously stronger than the dynamics, and the effect of the coupling model with the fractional operator model is better than that of the Hammerstein model.

Table 2: The root mean square error of the Hammerstein model and the proposed coupling model.

Frequency (f/Hz)	The root-mean-square error $e_{\mathrm{rms}}/(\mu m)$	
	The Hammerstein model	The proposed coupling model
1	0.4610	0.1787
10	0.4044	0.1174
20	0.3098	0.1106
50	0.3402	0.1482
100	0.2656	0.1932
5/40/80	0.1195	0.0682

Table 3: The relative error of the Hammerstein model and the proposed coupling model.

Frequency (f/Hz)	The relative error e_r	
	The Hammerstein model	The proposed coupling model
1	4.79%	1.86%
10	4.21%	1.22%
20	3.26%	1.16%
50	3.57%	1.55%
100	2.81%	2.05%
5/40/80	2.12%	1.21%

It can be clearly seen from Table 1 that in the case of ultralow frequency (1 Hz and below), the creep effect exhibits a differential nature. In addition, at other frequencies, the integral nature of the creep effect is characterized. In order to more clearly present the difference and effect between the proposed coupling model in this article and the Hammerstein model, two sets of quantitative indicators are given, namely, the root-mean-square error e_{rms} displayed in Table 2 and the relative error e_r described in Table 3. It can be clearly seen from Table 2 that the proposed coupling model of the fractional creep model in the series has a better effect, especially in the low-frequency range. On account of except for the hysteresis effect throughout the entire frequency range, the displayed creep effect is significantly higher than the dynamics characteristics, so the proposed coupling model is significantly better than the Hammerstein model. In the midrange frequency range, the effect of the coupling model is better because of the strong creep and dynamics characteristics. In the high-frequency range, the creep effect is gradually weakened, and the dynamics characteristic is the main property besides hysteresis. At this time, the Hammerstein model is obviously better than the low-frequency range. However, there is no doubt that the creep phenomenon cannot be ignored. The effect of the coupled model is still better than the Hammerstein model. In summary, the proposed coupling model in this paper can effectively describe the hysteresis, dynamics, and creep effects of the piezoelectric-actuated positioning stage; the relative error e_r is within about 2%.

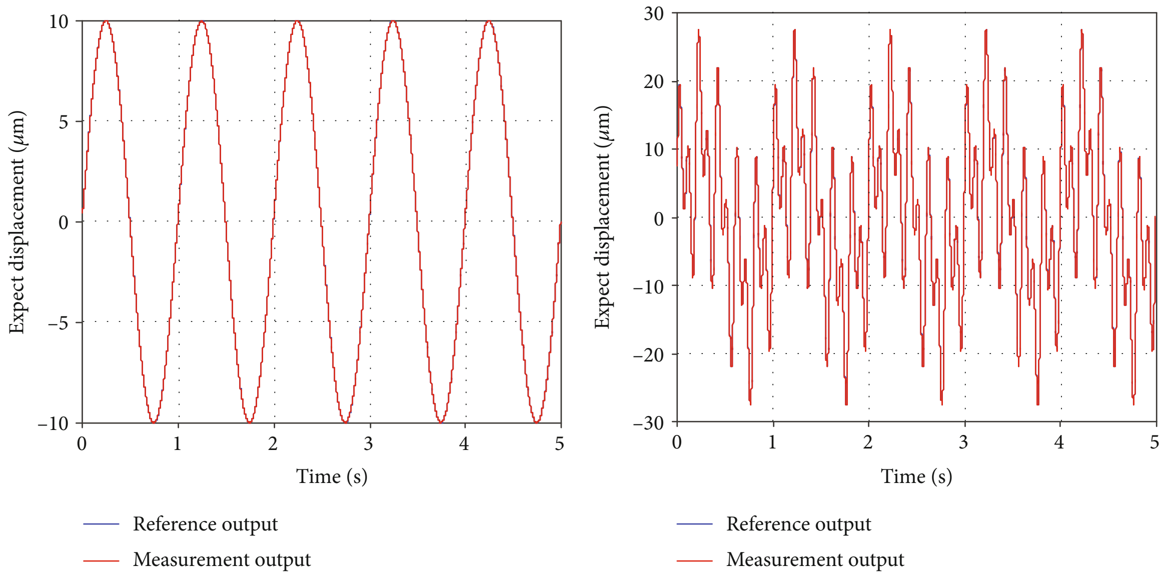

(a) $f = 1\,\text{Hz}$ (b) $f = 1\text{-}5\text{-}10\,\text{Hz}$

Figure 6: The tracking result of adaptive compound control.

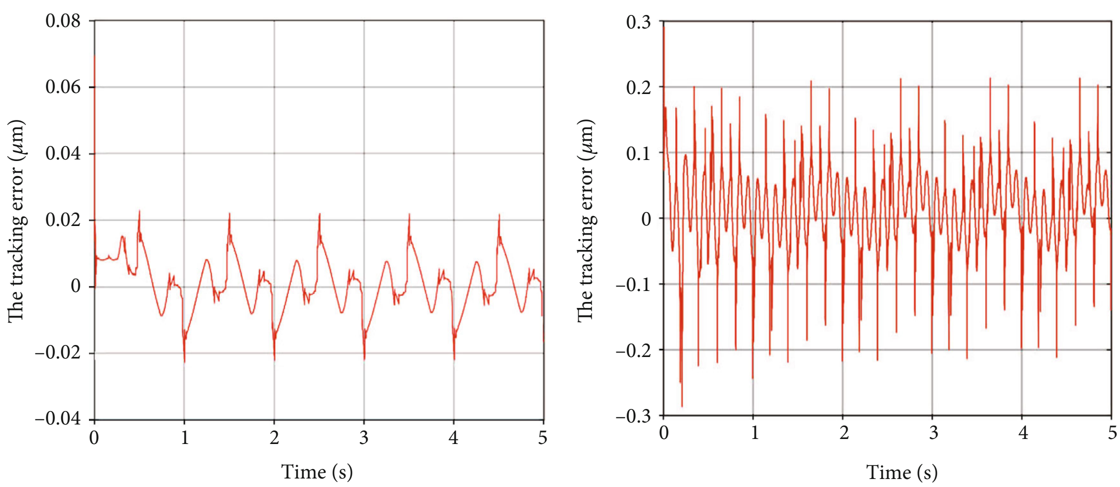

(a) $f = 1\,\text{Hz}$ (b) $f = 1\text{-}5\text{-}10\,\text{Hz}$

Figure 7: The tracking effect curve of adaptive compound control.

5.3. Analysis of Adaptive Control. In this paper, the input voltage signal is sinusoidal voltage signal $y_d(t) = 10 \sin(2\pi f t)$. The selected frequencies f are 1 Hz, 10 Hz, 20 Hz, and 50 Hz, and two sets of mixed frequency control input signals $y_d(t) = 10\sum_{i=1}^{3} \sin(2\pi f_i t)$. One set of frequencies are $f_1 = 1\text{Hz}$, $f_2 = 5\text{Hz}$, and $f_3 = 10\text{Hz}$; the other set of frequencies are $f_1 = 1\text{Hz}$, $f_2 = 10\text{Hz}$, and $f_3 = 20\text{Hz}$. The tracking control simulation is carried out.

Figure 6 shows the result of the adaptive control scheme, and Figure 7 shows the tracking error. It can be seen that the adaptive control scheme designed in this paper can track the expected displacement well in the case of mixing low and medium and low frequencies. Especially when the input signal frequency is 1 Hz, the tracking error is controlled around 0.02 μm.

It can be seen from the data in Tables 4 and 5 that the input-output tracking effect measured in the simulation study of adaptive compound control based on minimum variance is good. When the input signal is at low frequency 1 Hz, the creep characteristics are strong. The accuracy of the coupling model considering creep characteristics is obviously better than that of Hammerstein model without creep characteristics. However, with the increase of frequency, the positioning drift phenomenon becomes weaker, the calculus property of creep characteristics changes, and the influence of creep characteristics on the system is greatly weakened.

Table 4: The root mean square error of the adaptive compound control.

Frequency (f/Hz)	1	5	10
The root-mean-square error $e_{rms}/(\mu m)$	0.0076	0.0254	0.056
Frequency (f/Hz)	20	1/5/10	1/10/20
The root-mean-square error $e_{rms}/(\mu m)$	0.1153	0.0600	0.1787

Table 5: The relative error of the adaptive compound control.

Frequency (f/Hz)	1	5	10
The relative error e_r	0.11%	0.36%	0.80%
Frequency (f/Hz)	20	1/5/10	1/10/20
The relative error e_r	1.63%	0.49%	1.46%

Therefore, in this paper, the fractional operator parameters identified at 1 Hz are taken as the fractional creep model parameters in the simulation.

When the expected input signal frequency is 1 Hz, the root mean square errors e_{rms} based on the minimum variance adaptive composite control is 0.0076 μm. The relative error e_r is 0.76%. When the system input frequency is increased to the medium frequency, when the expected input signal frequency is 20 Hz, the root mean square error e_{rms} based on the minimum variance adaptive composite control is 0.1153 μm. The relative error e_r is 1.63%. In addition, when the input signal is a mixed frequency (1/5/10 Hz), the root mean square error e_{rms} of adaptive composite control based on minimum variance is 0.06 μm, and relative error e_r is 0.49%. Through the above data analysis, it can be seen that the minimum variance adaptive composite control can effectively track the expected input signal of the piezoelectric-driven positioning system, especially at low frequency.

6. Conclusion

In this paper, a new nonlinear model of coupled hysteresis, dynamics, and creep effects is proposed, which is based on the Hammerstein structure model and the fractional-order model. The Hammerstein model includes a classical PI model describing the static hysteresis characteristics and a second-order transfer function model representing the dynamic characteristics. The parameter identification of the proposed coupling model is simple and easy to implement. According to the coupling model, the feedforward compensations of the inverse of the fractional-order model and the inverse of the PI model are designed, and the tracking performance of the controlled system is adjusted by the adaptive control. To verify the effectiveness of the proposed model and controller, an experimental piezoelectric-actuated positioning stage is built. The experimental results show that the established coupling model can characterize accurately the complex nonlinear properties of the positioning stage. Also, the results show that the desired signal can be tracked well.

Data Availability

The data used to support the findings of this study are available from the corresponding author upon request.

Conflicts of Interest

The authors declare that they have no conflicts of interest.

Acknowledgments

This work was supported in part by the National Natural Science Foundation of China (U1813201, 62073297, and 61973157) and National Key Research and Development Project of China (2020YFB1712403).

References

[1] Y. F. Wang, R. Xu, and M. L. Zhou, "Prandtl-Ishlinskii modeling for giant magnetostrictive actuator based on internal time-delay recurrent neural network," *IEEE Transactions on Magnetics*, vol. 54, no. 11, pp. 1–4, 2018.

[2] F. J. Wang, J. L. Li, S. W. Liu, X. Y. Zhao, D. W. Zhang, and Y. L. Tian, "An improved adaptive genetic algorithm for image segmentation and vision alignment used in microelectronic bonding," *IEEE/ASME Transactions on Mechatronics*, vol. 19, no. 3, pp. 916–923, 2014.

[3] J. S. Kim, H. Youn, and B. Kang, "Ultra-precision 3 dof tilting stage for workpiece setup of scalable micro-pattern machining," *International Journal of Precision Engineering and Manufacturing*, vol. 18, no. 8, pp. 1103–1109, 2017.

[4] G. Y. Gu, L. M. Zhu, and C. Y. Su, "Modeling and compensation of asymmetric hysteresis nonlinearity for piezoceramic actuators with a modified Prandtl–Ishlinskii model," *IEEE Transactions on Industrial Electronics*, vol. 61, no. 3, pp. 1583–1595, 2014.

[5] L. Liu, H. Yun, Q. Li, X. F. Ma, S. L. Chen, and J. Shen, "Fractional order based modeling and identification of coupled creep and hysteresis effects in piezoelectric actuators," *IEEE/ASME Transactions on Mechatronics*, vol. 25, no. 2, pp. 1036–1044, 2020.

[6] R. Xu, X. Zhang, H. Guo, and M. Zhou, "Sliding mode tracking control with perturbation estimation for hysteresis nonlinearity of piezo-actuated stages," *IEEE Access*, vol. 6, pp. 30617–30629, 2018.

[7] G. Y. Gu, L. M. Zhu, C. Y. Su, H. Ding, and S. Fatikow, "Modeling and control of piezo-actuated nanopositioning stages: a survey," *IEEE Transactions on Automation Science and Engineering*, vol. 13, no. 1, pp. 313–332, 2016.

[8] Z. W. Zhu and X. Q. Zhou, "A novel fractional order model for the dynamic hysteresis of piezoelectrically actuated fast tool servo," *Materials*, vol. 5, no. 12, pp. 2465–2485, 2012.

[9] X. K. Chen, C. Y. Su, Z. Li, and F. Yang, "Design of implementable adaptive control for micro/nano positioning system driven by piezoelectric actuator," *IEEE Transactions on Industrial Electronics*, vol. 63, no. 10, pp. 6471–6481, 2016.

[10] K. Kuhnen and P. Krejci, "Compensation of complex hysteresis and creep effects in piezoelectrically actuated systems—a new preisach modeling approach," *IEEE Transactions on Automatic Control*, vol. 54, no. 3, pp. 537–550, 2009.

[11] Q. S. Xu and Y. M. Li, "Micro-/nanopositioning using model predictive output integral discrete sliding mode control," *IEEE*

Transactions on Industrial Electronics, vol. 59, no. 2, pp. 1161–1170, 2011.

[12] H. Hu, H. S. Zhang, and R. Ben Mrad, “Preisach based dynamic hysteresis model,” in *2004 International Conference on Intelligent Mechatronics and Automation, 2004. Proceedings*, pp. 825–830, Chengdu, China, August 2004.

[13] J. Z. Ge, L. Chang, and N. Prez-Arancibia, “Preisach-model-based position control of a shape-memory alloy linear actuator in the presence of time-varying stress,” *Mechatronics*, vol. 73, no. 5, pp. 1024–1031, 2021.

[14] M. Al Janaideh, S. Rakheja, and C. Y. Su, “An analytical generalized Prandtl–Ishlinskii model inversion for hysteresis compensation in micropositioning control,” *IEEE/ASME Transactions on Mechatronics*, vol. 16, no. 4, pp. 734–744, 2011.

[15] D. C. Jiles and D. L. Atherton, “Theory of ferromagnetic hysteresis (invited),” *Journal of Applied Physics*, vol. 55, no. 6, pp. 2115–2120, 1984.

[16] L. Li, G. Yang, and Q. Sun, “A hysteresis model considering temperature effects for sintered ndfeb and its application in electromagnetic buffer,” *Journal of Magnetism and Magnetic Materials*, vol. 537, article 168158, 2021.

[17] J. Sprekels and M. Brokate, “Hysteresis and phase transitions,” *Springer Science & Business Medi*, vol. 121, 1996.

[18] S. Shakiba, M. Ourak, E. V. Poorten, M. Ayati, and A. Yousefifi-Koma, “Modeling and compensation of asymmetric rate-dependent hysteresis of a miniature pneumatic artifificial muscle-based catheter,” *Mechanical Systems and Signal Processing*, vol. 154, no. 9, pp. 1152–1161, 2021.

[19] P. K. Wong, Q. S. Xu, C. M. Vong, and H. C. Wong, “Rate-dependent hysteresis modeling and control of a piezostage using online support vector machine and relevance vector machine,” *IEEE Transactions on Industrial Electronics*, vol. 59, no. 4, pp. 1988–2001, 2011.

[20] Y. F. Liu, J. J. Shan, and N. M. Qi, “Creep modeling and identification for piezoelectric actuators based on fractional-order system,” *Mechatronics*, vol. 23, no. 7, pp. 840–847, 2013.

[21] H. Jung and D. G. Gweon, “Creep characteristics of piezoelectric actuators,” *Review of Entifific Instruments*, vol. 71, no. 4, pp. 1896–1900, 2000.

[22] K. Kuhnen, “Modelling, identification, and compensation of complex hysteretic and log(t)-type creep nonlinearities,” *Control & Intelligent Systems*, vol. 33, no. 2, pp. 134–147, 2005.

[23] H. Janocha and K. Kuhnen, “Real-time compensation of hysteresis and creep in piezoelectric actuators,” *Sensors & Actuators A: Physical*, vol. 79, no. 2, pp. 83–89, 2000.

[24] G. Y. Gu and L. M. Zhu, “Motion control of piezoceramic actuators with creep, hysteresis and vibration compensation,” *Sensors & Actuators A: Physical*, vol. 197, no. 7, pp. 76–87, 2013.

[25] S. Das, *Functional Fractional Calculus for System Identification and Controls*, Springer, Berlin Heidelberg, 2008.

[26] S. K. Das, H. R. Pota, and I. R. Petersen, “High bandwidth multi-variable combined resonant and integral resonant controller for fast image scanning of atomic force microscope,” in *2013 IEEE/ASME International Conference on Advanced Intelligent Mechatronics*, pp. 838–843, Wollongong, NSW, Australia, July 2013.

[27] X. Zhang, B. Li, Z. Li, C. Yang, X. Chen, and C.-Y. Su, “Adaptive neural digital control of hysteretic systems with implicit inverse compensator and its application on magnetostrictive actuator,” *IEEE Transactions on Neural Networks and Learning Systems*, vol. 33, no. 2, pp. 667–680, 2022.

[28] L. Cheng, W. Liu, Z. G. Hou, T. Huang, J. Yu, and M. Tan, “An adaptive Takagi-Sugeno fuzzy model-based predictive controller for piezoelectric actuators,” *IEEE Transactions on Industrial Electronics*, vol. 64, no. 4, pp. 3048–3058, 2017.

[29] X. K. Chen, T. Hisayama, and C. Y. Su, “Adaptive control for uncertain continuous-time systems using implicit inversion of prandtl-ishlinskii hysteresis representation,” *IEEE Transactions on Automatic Control*, vol. 55, no. 10, pp. 2357–2363, 2010.

[30] Y. Q. Chen, I. Petras, and D. Y. Xue, “Fractional order control - a tutorial,” in *2009 American control conference*, pp. 1397–1411, St. Louis, MO, USA, June 2009.